Mon. Not. R. Astron. Soc. **000**, ??–?? (2011) Printed 10 March 2012 (MN LATEX style file v2.2)

A Spatial FFT and FX Correlator for the BEST-2 Array

G. Foster[1], J. Hickish[1], D. Price[1], K. Zarb Adami[1]
[1] *Oxford University, Department of Physics*

10 March 2012

ABSTRACT
A new FX correlator and a spatial FFT imager has been developed using CASPER FPGA hardware for the BEST-2 array at the Radiotelescopi di Medicina in Italy. Both instruments use the same digitizing/channelizing front end. The spatial FFT imager takes advantage of BEST-2 as a regularly gridded array to perform a 2D spatial FFT using $O(n \log n)$ operations. The FX correlator has been used to solve complex gain calibrations which are applied in the spatial FFT during observation. During the initial deployment of the instruments several bright radio sources were observed over multiple epochs.

1 INTRODUCTION

The Basic Element for SKA Training (BEST) 2 array is a subset of the Northern Cross cylindrical array, at the Radiotelescopi di Medicina in Italy. In this paper we describe a new digital backend designed for this array, implemented on CASPER (Parsons et al. 2006) designed FPGA-based hardware, and comprising fast correlation, direct imaging, beamforming and transient processing capabilities.

These instruments have been installed as prototypes for larger scale instruments currently in development. The correlator is being used to study the handling of large output data rates and the development of real time millisecond imaging using many antenna elements. The direct imaging system is being used to study the feasibility of such systems in arrays with regular geometric structure, as well as providing a platform for pulsar surveys and space-debris tracking capabilities with BEST-2. Since deployment, a number of sources with the correlator and imager have been successfully observed. Data has been reduced and calibrated using a combination of custom software and standard radio synthesis imaging packages.

In the first section of this paper we give an overview of the BEST-2 Array, followed by a description of the channelization, correlation and image-domain processing systems in Sections 2.1, 2.2 and 2.3, respectively. Results from preliminary observations of bright radio sources from these systems are presented in Section **??**, with a discussion of these in Section 4.

1.1 BEST-2 Array

The BEST-2 testbed at the Medicina Radio Observatory consists of 8 East-West oriented cylindrical concentrators, each with 64 dipole receivers critically sampling for focal line at 408MHz. These 64 dipoles are summed in groups of 16, resulting in 4 channels per cylinder, and a total of 32 effective receiving elements laid out on a *4-by-8* grid, fig. 1.

BEST-2 was developed as a reliable, low cost frontend to be used in SKA development, with simplicity of interfacing with different digital backends a core design requirement (Montebugnoli et al. 2009b). Extensive documentation of the development of the BEST-2 analogue chain can be found in a number of papers (Perini 2009) (Perini et al. 2009). The top level specifications of the array are shown in table 1.

In 2008 the initial digital correlator backend of the array was based on iBOB and BEE2 FPGA boards from the Collaboration for Astronomy Signal Processing and Electronics Research (CASPER)(Montebugnoli et al. 2009a). An upgraded digital backend has been developed using the ROACH board, also developed by CASPER, which includes an FX correlator, spatial FFT imager and beamformer.

2 INSTRUMENT DESIGN

An FX correlator and spatial FFT imager instrument have been built for BEST-2. Both instruments use the same digitization and channelization frontend. This allow a streamlined process of calibrating the spatial FFT imager, reduces the amount of

BEST-2 Array Specifications		
Cylinder & Element Properties		
Number of RX per Cylinder	4	
Cylinder Diameter	7.5	m
Cylinder Length	23.5	m
Element Diameter	7.5	m
Element Length	5.88	m
Element Collecting Area	44.1	m^2
Aperture Efficiency	0.71	
Element Effective Area	31.3	m^2
BEST-2 Array Properties		
Number of Cylinders	8	
Total Number of RX	32	
Total Collective Area	1411.2	m^2
Total Effective Area	1001.95	m^2
Sensitivity / Ant. gain	0.36	K/Jy
A_{eff}/T_{sys}	11.65	m^2/K
Antenna Temperature	35	K
Receiver Temperature	51	K
System Temperature	86	K
Longest Baseline		
E-W	17.04	m
N-S	70.00	m
Bandpass		
Central Frequency	408	MHz
Analog Bandwidth	16	MHz
Pointing Limits		
Declination	(0,+90)	deg
Right Ascension	Local Meridian	
Primary Beam		
Primary Beam Size	37.62	deg^2
Declination	5.7	deg
Right Ascension	6.6	deg
PSF		
PSF FWHM	0.9	deg^2
Declination	0.52	deg
Right ascension	1.73	deg

Table 1. The top level specifications of the BEST-2 Array, a subset of the collecting area of the Northern Cross, located in Medicina, Italy.

hardware and allows for simultaneous observation with both instruments. The instrument has been implemented on ROACH boards which are a generic field programmable gate array (FPGA) board designed by CASPER for radio astronomy applications. A ROACH consist of a XILINX Virtex 5 SX95T FPGA with interfaces to DRAM and QDR memory, high speed CX-4 connectors and a generic Z-DOK interface for connecting ADCs and various daughter boards, fig 2. Additionally, the board has a PowerPC running BORPH, a variant of Debian Linux, which allows access to software registers and shared memory on the FPGA. Firmware is designed using MATLAB Simulink which is extended with XILINX DSP blocks and CASPER's open source DSP blocks(). Design specific DSP blocks and hardware interfaces have also created, design models and control

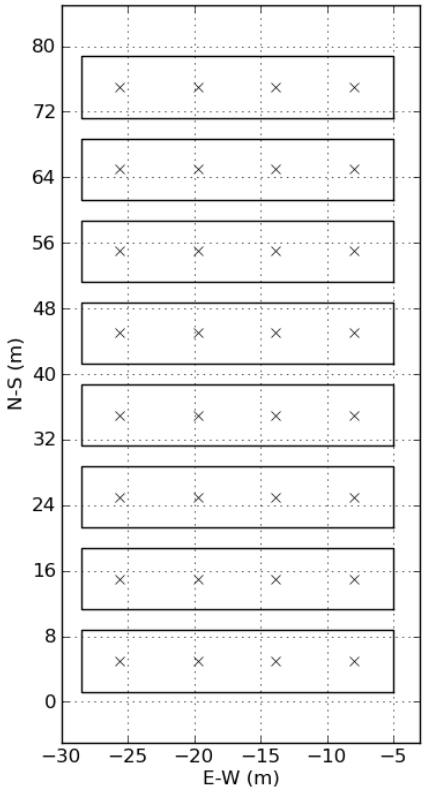

Figure 1. The 32 effective receiving elements of BEST-2, indicated by crosses, lie on a regular 4x8 grid. Each receiver is the analogue sum of 16 dipoles, critically spaced at 408MHz in the East-West direction.

software are available from our project repository[1]. Instrument design specifications are presented in table 2, further design detail is described in the following sections.

2.1 Digitization and Channelization

Signal digitization is performed using the Texas Instruments ADS5272 8 channel, 12 bit ADC. The ADC board, developed by Rick Raffanti (), uses eight of these ADCs to channelize 64 streams at up to 65 Msps. In our design only 32 signal streams are digitized at 40 Msps which more then covers the 16 MHz analog band. The ADC is clocked with a 160 MHz clock which is locked to a local maser source. During the analog stage the RF, centered at 408 MHz, has been mixed down to baseband. Prior to digitization the last amplifier stage of the analog chain has per signal adjustable gain useful for setting good levels for ADC quantization. This ADC is connected via a dual Z-DOK interface to an 'F-Engine' ROACH which performs the channelization. The ROACH board is clocked at four times the sample rate such that four signals are time division multiplexed onto a single stream. Channelization is performed with a four tap Hann filter, 2048 point polyphase filterbank (PFB) to produce 1024 samples per real antenna stream. The CASPER PFB has been modified to account for the signal multiplexing. Each channel has a width of 19.5 kHz and the output of the FFT stage is a 36 bit complex number. The narrow channel widths and PFB windowing allows for good frequency separation in the high RFI environment at the observatory. After channelization the samples are quantized down to a 8 bit complex number. An adjustable, per channel complex gain equalizer is used for amplitude and phase corrections before quantization. Complex gain calibration is essential to proper spatial FFT imaging which must be applied before the spatial FFT. The FX correlator is used to generate calibration coefficients which are applied back into the equalizers. A selectable mux is available to skip the phase coefficients on the FX correlator data stream. Post equalization the data stream is split into two for specific reordering for the correlator and imager. The correlator data stream is reordered to 128 time samples for a single antenna for a single frequency channel. Followed by the next antenna and cycles

[1] https://github.com/griffinfoster/medicina

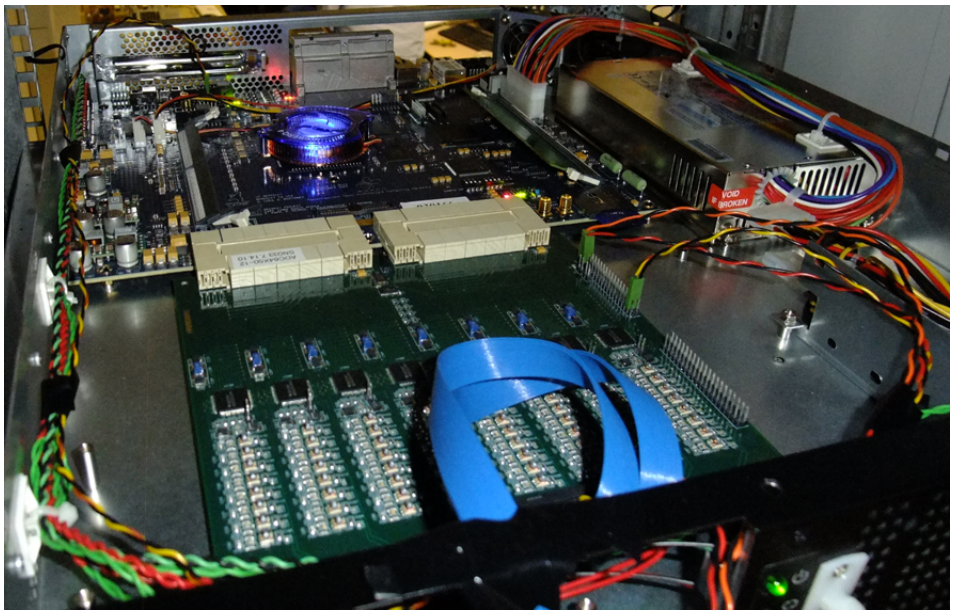

Figure 2. The 'f-engine' ROACH board, a Virtex 5 SX95T FPGA board, with the 64 input ADC connected via two Z-DOK connectors.

Digital Backend Specifications		
Digitizer/Channelizer (F-Engine)		
ADC Sampling Rate	40	MHz
ADC Sampling Precision	12	bit
Antenna-polarizations	32	single pol
PFB	4 tap FIR + 2048 point FFT	Radix-2 Biplex Real FFT
Quantization	4	bit
FX Correlator (X-Engine)		
Auto Correlations	32	
Cross Correlations	496	
Minimum Integration Length	6.55	ms
Output	10 GbE	SPEAD protocol
Spatial FFT Imager (S-Engine)		
2D FFT	8 x 16	
Beams	128	
Minimum Integration Length	1	s
Output	1 GbE	SPEAD protocol
Beamformer Output	10 GbE	Up to 8 Beams

Table 2. A three ROACH design where the correlator and spatial FFT imager use the digitizer/channelizer interface.

back onto the next frequency channel. The imager takes in one time sample of each antenna for a given frequency channel and cycles through 128 time samples before stepping to the next frequency channel. After data reordering each stream is sent over high speed XAUI at a rate of 5.12 Gbps to the correlator and imaging boards.

2.2 FX Correlator

An FX correlator design is a standard design for large bandwidth and many antenna arrays. The F component represents the frequency channelization, and the X is a complex multiply and accumulate (CMAC). An overview of the architecture is presented in (). Architecture efficiency goes as $O(M\log M)+O(N^2)$ where M is the number of FFT frequency channels and N is the number of antenna-polarizations. The core component to the X stage of the FX correlator is the complex multiplication

F-Engine ROACH Resource Utilization (Virtex 5 SX95T)		
ADC Clock	40 MHz	
System Clock	160 MHz	Demux:4
Slice Registers	30217 / 58880	51%
Look Up Tables	24319 / 58880	41%
BRAM (36kb)	205 / 244	84%
DSP48e (Multipliers)	185 / 640	28%
CX-4 Interface	2 / 4	5.12 Gbps XAUI
QDR Memory	2 / 2	Cornerturn

Table 3. DSP implementation of the 'f-engine'

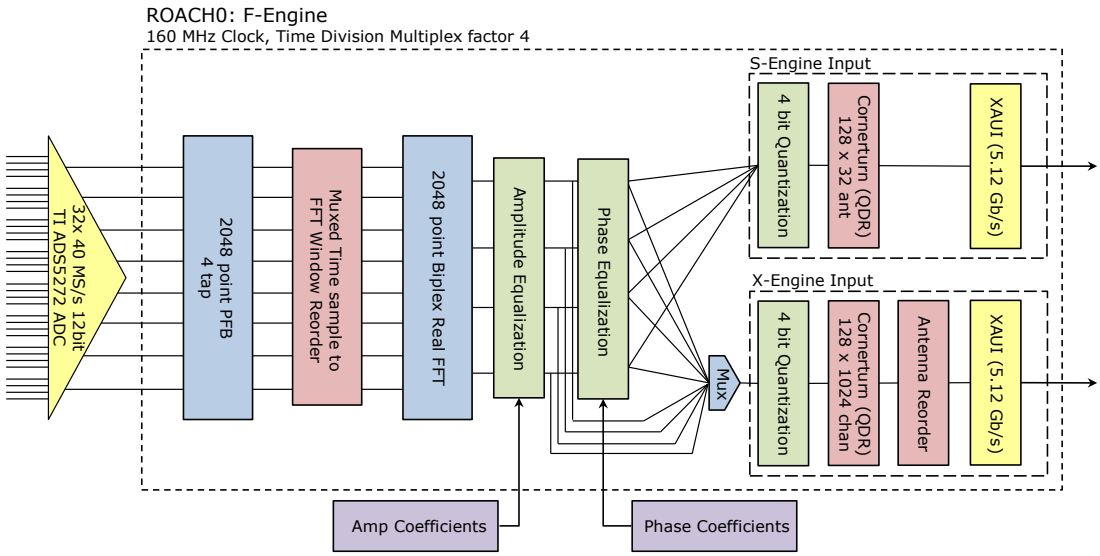

Figure 3. During observations amplitude and phase coefficients are applied to scale the power for the 4 bit correlation and apply phase corrections for the spatial FFT.

of all pairs of independent signals for each frequency channel. A pipelined x-engine, based on the general CASPER block originally designed by Lynn Urry(), is used for multiplier efficiency. The pipeline design is constructed out of $M/2$ 'taps' where the i^{th} tap computes the correlation between antennas A_j and A_{j+i} for every antenna A_j of M total antennas. To maximize the multiplier usage a loopback is added to use every i^{th} tap to compute the correlation of antennas A_j and $A_{M/2+j+i}$, fig. 4. Each tap accumulates for N time samples to reduce the output data rate.

An asynchronous architecture is used between the f-enigne and x-engine boards. The x-engine board has been clocked to

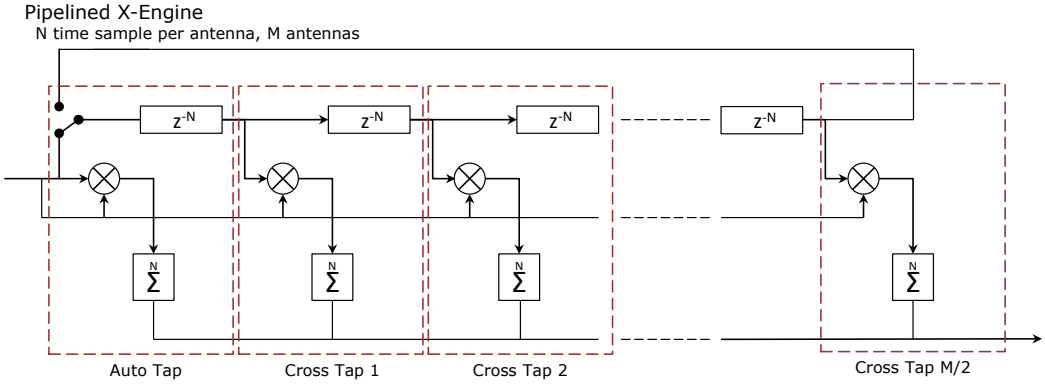

Figure 4. The input is ordered as N time samples per antenna per frequency channel. An accumulation stage after the complex multiply reduces the data rate of each tap. Outputs are multiplexed onto the same output using a valid signal.

X-Engine ROACH Resource Utilization (Virtex 5 SX95T)		
System Clock	200 MHz	
Slice Registers	28494 / 58880	48%
Look Up Tables	25349 / 58880	43%
BRAM (36kb)	88 / 244	36%
DSP48e (Multipliers)	288 / 640	45%
CX-4 Interface	1 / 4	5.12 Gbps XAUI
QDR Memory	2 / 2	Vector Accumulator

Table 4. DSP implementation of the 'x-engine'

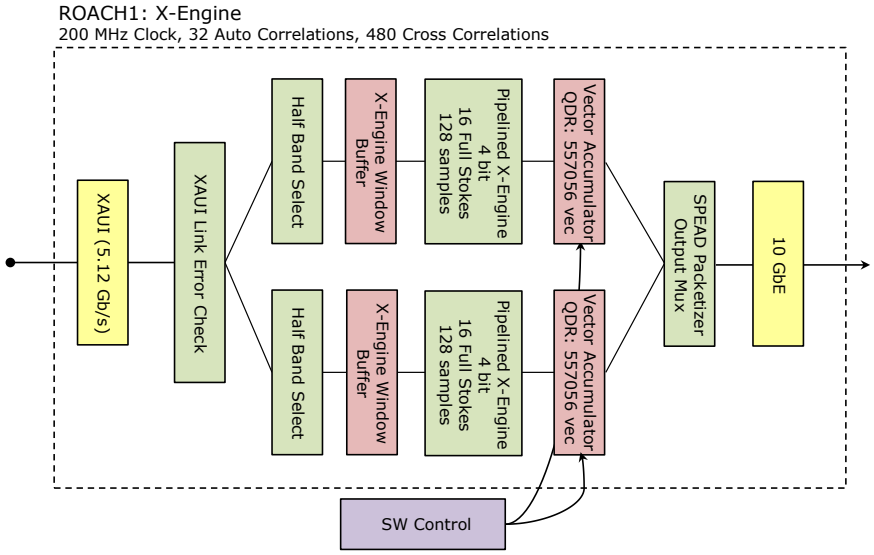

Figure 5. Two parallel pipelined x-engines are used, each processes half of the band.

200 MHz, well above the 160 MHz f-engine board, this assures the x-engine board will never have input buffer overflows during the windowing stage. The XAUI interboard connection is a streaming interface which guarantees the same output order as input order but with variable latency. In rare cases the XAUI interface can drop 64 bit words during the streaming, this requires an initial stage to track the number of words received between headers. In case of missing words the entire payload is dropped and counters reset for the next header. A correlation is only performed on a per channel basis. The channelized band can be split up into portions and processed in parallel across multiple x-engines. This allows a larger bandwidth to be processed at the cost of increased logic and multiplier resource utilization. For this design two x-engines are used which each processes half of the band. The x-engine design requires a continuous stream of data for 128 samples of all antennas for a single frequency channel. Prior to the x-engine samples are buffered up into windows to guarantee valid data during a cycle of the x-engine. For reasons related to the design the 32 single polarization signals are treated as 16 dual polarization signals. This causes a small number of redundant baseline correlations and a conjugation effect which is corrected in post processing. During the x-engine stage an initial accumulation of 128 sample is performed after the complex multiply to reduce the output rate to roughly the input rate. This limits the minimum integration time to 6.55 ms. A vector accumulator using the on board QDR memory is used for longer integration lengths. This second accumulator is software controlled with integration lengths ranging from milliseconds to minutes. A completed integration is sent to a receive computer over a 10 GbE connection. Integrations are split up based on the SPEAD protocol() and transmitted as UDP packets.

2.3 Spatial FFT

When N receiving elements in an antenna array are placed on a regularly spaced grid, a well known method for producing a complete set of orthogonal beams on the sky is the spatial fast Fourier transform (Williams 1968). Such a beamforming implementation will generate N beams on the sky, with a computational cost of $O(N \log N)$. For large arrays, where many beams are desired, this can be a significant computational saving, with the alternative, so-called *DFT beamforming*, requiring

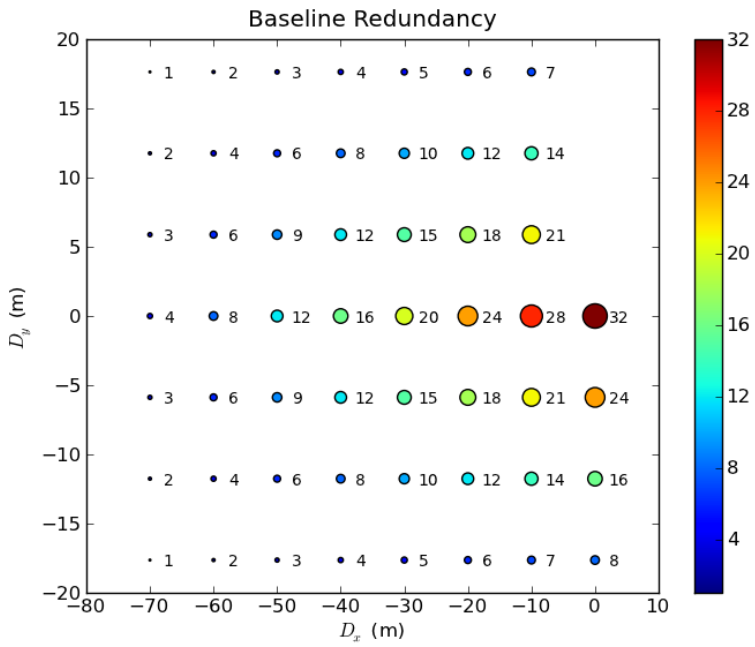

Figure 6. A 4 by 8 regularly gridded array has 52 unique baselines, 480 cross correlations are performed. The number of redundant baseline measurements is shown as the color and size of each circle.

$O(N)$ operations per synthesized beam. To date, the largest such astronomical implementation of such a spatial fast Fourier transform beamformer is the 64 element dish array constructed in 1994 at Waseda University, Japan (Otobe et al. 1994).

More recently, spatial FFT based processing has been revisited in the literature with an emphasis on the correlation matrix, rather than the collection of beams, as the mathematical object of interest (Tegmark & Zaldarriaga 2009) (Tegmark & Zaldarriaga 2010). In the method outlined by Tegmark & Zaldarriaga, zero padding is applied to the matrix of antenna signals before the spatial FFT is performed, and as such, the complete set of visibilities for all unique baselines in the array can be obtained, post integration, by inverse Fourier transform. Conversely, in the image plane, the zero-padding required by the prescribed algorithm results in the generation of $2^m N$ beams on the sky and is dependent on the number of dimensions, m, in the antenna array. Regardless of potential downstream visibility domain processing, this oversampling of the sky by a factor 2^m has the benefit of increasing the instantaneous uniformity of sky coverage by synthesized beams, which somewhat alleviates the limitations associated with the inability to steer multiple beams independently.

In the BEST-2 backend described here, the requirements on the spatial FFT processor were multifold. Firstly, the system should be capable of generating images on an O(second) timescale, by the method described by (Tegmark & Zaldarriaga 2009). Further, the system should be capable of passing formed beams at full bandwidth, i.e. without any accumulation, to downstream time domain processing systems such as the real-time dedispersion engine (Magro et al. 2011).

This redundancy for the BEST-2 array is show in figure 6. Instead of making individual correlations of the same baseline as in an FX correlator the correlation of the average of each baseline can be computed. This optimization realizes on the assumption that each redundant baseline measurement is indeed identical. Thus any calibration to the complex gains must be applied before the spatial FFT.

Though the X-Engine and S-Engine use the same F-Engine each requires a unique data windowing order. For the S-Engine a window is made up of N antennas by M time samples for a given frequency channel. A similar XAUI interface and windowing scheme is used as in the X-Engine which buffers up windows of valid data to stream into the spatial transform. The 2D spatial transform is performed using an 8 point FFT followed by a cornerturn and 16 point FFT. The BEST-2 array is a grid of 4 by 8 antennas, the data is zero padded before input into the 8 by 16 point spatial transform. A 4 by 8 point spatial transform will only produce gain information for each spatial position, which can be interpreted as an array of beamformers covering the field of view. This zero padding is necessary to produce both the gain and phase information of each spatial position which is an effective baseline. Each effective baseline is an average of all possible baselines with the same spatial dimensions. The four fold increase is the number of outputs from the spatial transform by double padding introduces a number of redundant calculations. The spatial transform produces 128 outputs, there are only 53 unique baselines in a 4 by 8 grid. The datarate out of the S-Engine is reduced by a two stage vector accumulator. A fixed 128 sample vector accumulator reduces the output of the second stage FFT so that the 1024 channels of the 128 computed spatial components can be multiplexed onto one line

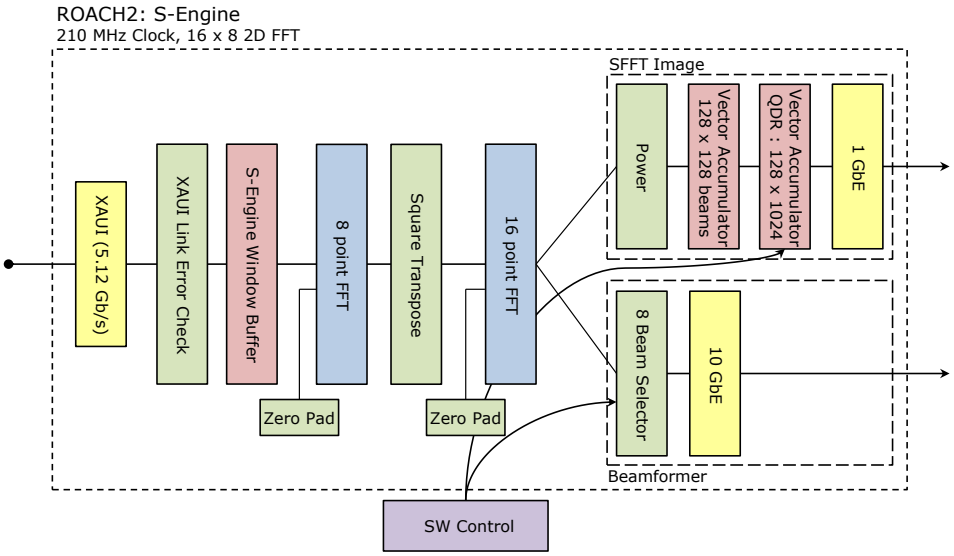

Figure 7. During the two stage spatial FFT the streams are zero padded to provide phase information of each baseline.

and accumulated in a software controllable QDR vector accumulator. Accumulations are sent out over the 1 GbE PowerPC interface using the a SPEAD UDP packet format. Individual beams can be selected out before accumulation and sent over 10 GbE in a LOFAR beam packet format which will be used for future pulsar processing.

3 DEPLOYMENT AND INITIAL OBSERVATIONS

Instrumentation was installed and tested over a two week period in March 2012. During that time a number of test signals were used to check the system status. Once the system was checked out various bright radio sources were observed. Since the Northern Cross is a transiting array there is a limited period of time each day in which a source is with the primary beam. Bright sources such as Cygnus A, Cassiopeia A and Virgo A also with a number of 3C sources were observed along with multiple constant declination 24 hour cycles were observed.

Raw data from the correlator and imager was recorded to HDF5 files using a SPEAD protocol receive script. A suite of python scripts have been written to interface and manipulate the data in this pre-calibration stage. A python FITS-IDI package has been written to convert HDF5 files into the standard FITS format which can be read by AIPS and CASA[2]. This allows for conversion to the Measurement Set format which most packages can interface with.

A number of calibration methods has been tested on the initial data sets. Traditional CASA based calibration has been used to form correlator images. To produce calibration coefficients for the spatial FFT imager a column ratio gain estimation method has been employed. A study of the baseline redundancy and possible calibration has also been undertaken. Long observations of the sky are under way to understand the system noise and our ability to reach the confusion limit. During deep integration observations a cross talk issue covering part of the band has been discovered.

3.1 Calibration Methods

The effective averaging of redundant baselines in the spatial FFT imager requires complex gain calibrations to be applied during observations. To derive gain coefficients a calibration method is applied to the FX correlator data. In initial observations the column ratio gain estimation method from (Boonstra & Veen 2001) was used to compute a per channel, per antenna complex gain term.

3.2 FX Correlator Imaging

The East-West FWHM beam size of an individual element is 6.6° which translates to a 26 minute 'transit time' for an source. For the the bright A class sources this time can be extended since they remain the dominating source well after crossing

[2] https://github.com/telegraphic/pyfitsidi

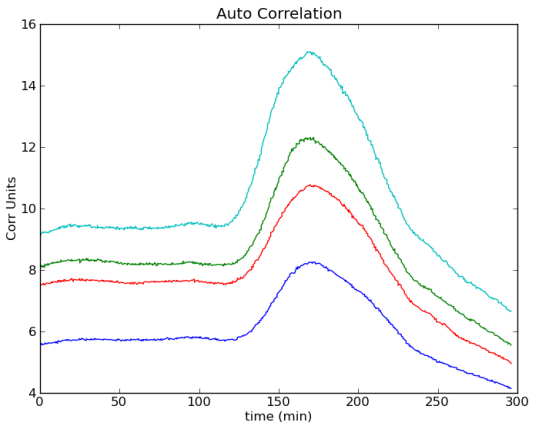

(a) A selection of typical auto correlations over a period of five hours during a transit of Cygnus A. The asymmetry is due to the background galactic plane.

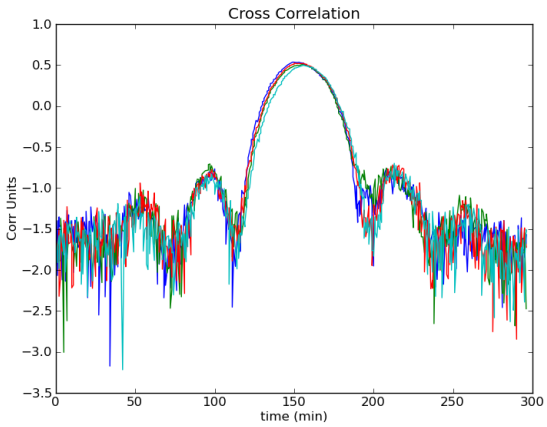

(b) Cross correlation power over a period of five hours during a Cygnus A transit. The first sidelobes are around 100 times lower then the primary lobe. A bright source like Cygnus A remains the dominant source in the field even into the second sidelobe.

Figure 8. Typical auto and cross correlations of a transiting source.

the FWHM. Observations of 40-50 minutes are possible which gives an improvement in uv coverage. Initial calibration and imaging has been performed using the bright sources: Cygnus A, Cassiopeia A, Virgo A and Taurus A.

A transiting array provides a unique challenge of gain calibration since a source's apparent gain will change as it transits the primary beam. A typical beam transit of a strong source, Cygnus A, is show in figure **??**. The auto correlations asymmetry is due to the changing galactic plane pass through the beam. In the cross correlations the first and second sidelobes are evident. Much of the sky surrounding a bright source is contaminated due to these high sidelobes. The traditional method of using a gain calibrator is not possible. Gain calibration of bright sources was done by fitting a solution on short time intervals. A model of the beam will be necessary to set a better flux scale and time independent gain solution.

3.3 Spatial FFT Results

3.4 Comparison of FX Correlator and Spatial FFT

4 DISCUSSION

REFERENCES

Boonstra A. J., Veen A. J. V. D., 2001, in IEEE Workshop on Statistical Signal Processing (SSP), IEEE

Magro A., Karastergiou A., Salvini S., Mort B., Dulwich F., Zarb Adami K., 2011, MNRAS, 417, 2642

Montebugnoli S., Bartolini M., Bianchi G., Naldi G., Manley J., Parsons A., 2009a, in Proceedings of Wide Field Astronomy & Technology for the Square Kilometre Array (SKADS 2009). 4-6 November 2009. Chateau de Limelette, Belgium, pp. 355–358

Montebugnoli S., Bianchi G., Monari J., Naldi G., Perini F., Schiaffino M., 2009b, in Proceedings of Wide Field Astronomy & Technology for the Square Kilometre Array (SKADS 2009). 4-6 November 2009. Chateau de Limelette, Belgium, pp. 331–336

Otobe E. et al., 1994, Publications of the Astronomical Society of Japan, 46, 503

Parsons A. et al., 2006, in Asilomar Conference on Signals and Systems, Pacific Grove, CA, pp. 2031–2035

Perini F., 2009, in Proceedings of Wide Field Astronomy & Technology for the Square Kilometre Array (SKADS 2009). 4-6 November 2009. Chateau de Limelette, Belgium., pp. 341–345

Perini F., Bianchi G., Schiaffino M., Monari J., 2009, in Proceedings of Wide Field Astronomy & Technology for the Square Kilometre Array (SKADS 2009). 4-6 November 2009. Chateau de Limelette, Belgium, pp. 351–354

Tegmark M., Zaldarriaga M., 2009, Phys. Rev. D, 79, 083530

Tegmark M., Zaldarriaga M., 2010, Phys. Rev. D, 82, 103501

Williams J. R., 1968, The Journal of the Acoustical Society of America, 44, 1454